



**HAL**  
open science

## Twenty-five years of geodetic measurements along the Tadjoura-Asal rift system, Djibouti, East Africa

Christophe Vigny, Jean-Bernard de Chabalier, Jean-Claude Ruegg, Philippe Huchon, Kurt L. Feigl, Rodolphe Cattin, Laike Asfaw, Khaled Kanbari

### ► To cite this version:

Christophe Vigny, Jean-Bernard de Chabalier, Jean-Claude Ruegg, Philippe Huchon, Kurt L. Feigl, et al.. Twenty-five years of geodetic measurements along the Tadjoura-Asal rift system, Djibouti, East Africa. *Journal of Geophysical Research: Solid Earth*, 2007, 112; B2, pp.B06410. 10.1029/2004JB003230 . insu-01288905

**HAL Id: insu-01288905**

**<https://insu.hal.science/insu-01288905v1>**

Submitted on 15 Mar 2016

**HAL** is a multi-disciplinary open access archive for the deposit and dissemination of scientific research documents, whether they are published or not. The documents may come from teaching and research institutions in France or abroad, or from public or private research centers.

L'archive ouverte pluridisciplinaire **HAL**, est destinée au dépôt et à la diffusion de documents scientifiques de niveau recherche, publiés ou non, émanant des établissements d'enseignement et de recherche français ou étrangers, des laboratoires publics ou privés.

## Twenty-five years of geodetic measurements along the Tadjoura-Asal rift system, Djibouti, East Africa

Christophe Vigny,<sup>1</sup> Jean-Bernard de Chabali er,<sup>2</sup> Jean-Claude Ruegg,<sup>2</sup> Philippe Huchon,<sup>3</sup> Kurt L. Feigl,<sup>4</sup> Rodolphe Cattin,<sup>1</sup> Laike Asfaw,<sup>5</sup> and Khaled Kanbari<sup>6</sup>

Received 14 June 2004; revised 12 December 2006; accepted 18 December 2006; published 19 June 2007.

[1] Since most of Tadjoura-Asal rift system sits on dry land in the Afar depression near the triple junction between the Arabia, Somalia, and Nubia plates, it is an ideal natural laboratory for studying rifting processes. We analyze these processes in light of a time series of geodetic measurements from 1978 through 2003. The surveys used triangulation (1973), trilateration (1973, 1979, and 1981–1986), leveling (1973, 1979, 1984–1985, and 2000), and the Global Positioning System (GPS, in 1991, 1993, 1995, 1997, 1999, 2001, and 2003). A network of about 30 GPS sites covers the Republic of Djibouti. Additional points were also measured in Yemen and Ethiopia. Stations lying in the Danakil block have almost the same velocity as Arabian plate, indicating that opening near the southern tip of the Red Sea is almost totally accommodated in the Afar depression. Inside Djibouti, the Asal-Ghoubbet rift system accommodates  $16 \pm 1$  mm/yr of opening perpendicular to the rift axis and exhibits a pronounced asymmetry with essentially null deformation on its southwestern side and significant deformation on its northeastern side. This rate, slightly higher than the large-scale Arabia-Somalia motion ( $13 \pm 1$  mm/yr), suggests transient variations associated with relaxation processes following the Asal-Ghoubbet seismovolcanic sequence of 1978. Inside the rift, the deformation pattern exhibits a clear two-dimensional pattern. Along the rift axis, the rate decreases to the northwest, suggesting propagation in the same direction. Perpendicular to the rift axis, the focus of the opening is clearly shifted to the northeast, relative to the topographic rift axis, in the “Petit Rift,” a rift-in-rift structure, containing most of the active faults and the seismicity. Vertical motions, measured by differential leveling, show the same asymmetric pattern with a bulge of the northeastern shoulder. Although the inner floor of the rift is subsiding with respect to the shoulders, all sites within the rift system show uplift at rates varying from 0 to 10 mm/yr with respect to a far-field reference outside the rift.

**Citation:** Vigny, C., J.-B. de Chabali er, J.-C. Ruegg, P. Huchon, K. L. Feigl, R. Cattin, L. Asfaw, and K. Kanbari (2007), Twenty-five years of geodetic measurements along the Tadjoura-Asal rift system, Djibouti, East Africa, *J. Geophys. Res.*, *112*, B06410, doi:10.1029/2004JB003230.

### 1. Introduction

[2] The Afar depression, at the triple junction between Arabia, Somalia, and Nubia, is actively deforming by continental stretching, rifting, and volcanism. Here, the three extensional structures of the Sheba Ridge, the Red Sea Ridge, and the East African Rift join in a complicated

geometry. Both the Red Sea Ridge and Sheba Ridge have been propagating for the last 30 Ma, toward the south and west, respectively. Yet they penetrate into the Afar depression, rather than connecting directly through the Straits of Bab el Mandeb. Consequently, the recent tectonic action there focuses around a set of disconnected, but overlapping, propagating rift segments that have created a complex network of normal faults [e.g., Huchon *et al.*, 1991; Dauteuil *et al.*, 2001; Manighetti *et al.*, 1997]. To better understand the kinematics and the processes taking place in this area, we use geodetic measurements to characterize the deformation at three scales defined by different geophysical objects: the plates (distances  $\sim 1000$  km), tectonic regions (between  $\sim 1000$  km and  $\sim 10$  km), and rift segments ( $\sim 10$  km).

[3] At the scale of the plates, the existing long-term kinematic models disagree markedly. The conventional NUVEL-1A model considers Africa as a single plate to predict divergence between Africa and Arabia at a rate of

<sup>1</sup>Laboratoire de G eologie, Ecole Normale Sup erieure, CNRS, Paris, France.

<sup>2</sup>Institut de Physique du Globe, Paris, France.

<sup>3</sup>Laboratoire de Tectonique, Universit e Pierre et Marie Curie-Paris 6 and Institut O c anographique, Paris, France.

<sup>4</sup>Department of Geology and Geophysics, University of Wisconsin-Madison, Madison, Wisconsin, USA.

<sup>5</sup>Addis Observatory, Department of Geophysics, Addis Ababa University, Addis Ababa, Ethiopia.

<sup>6</sup>Department of Geosciences, University of Sana'a, Sana'a, Yemen.

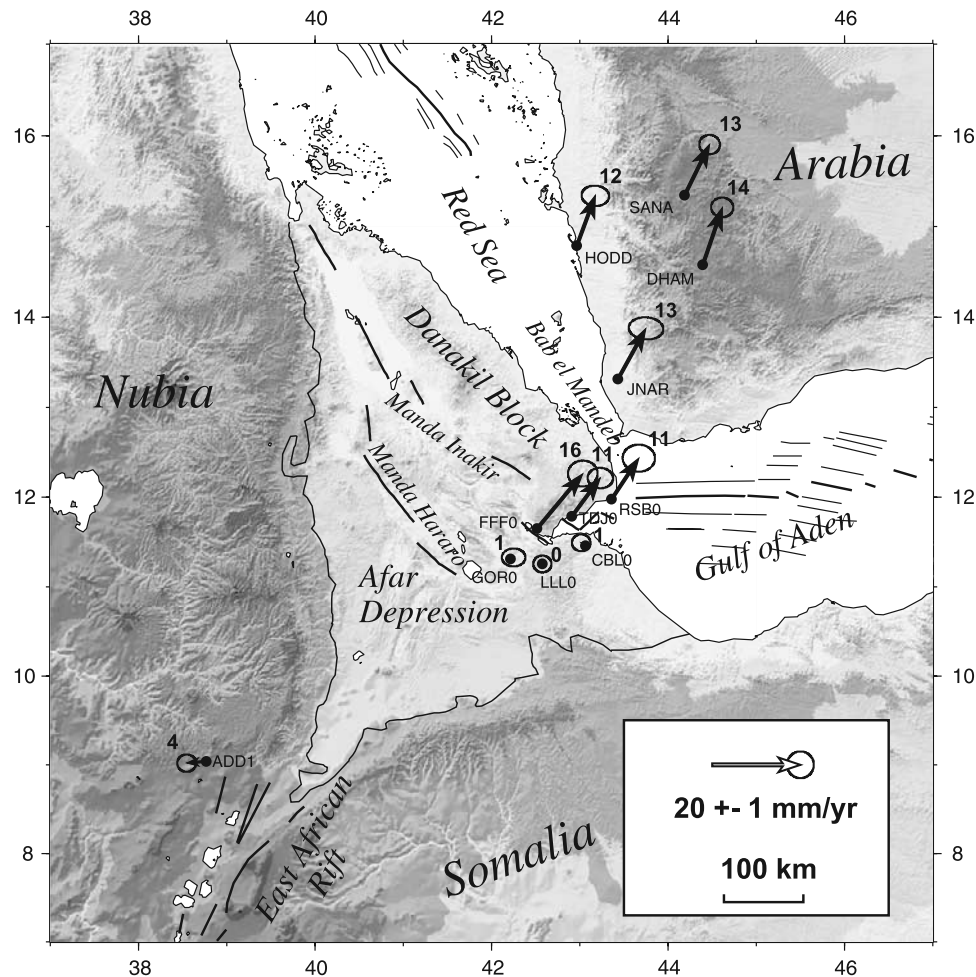


**Figure 1.** Triple junction and Afar depression. Dots show locations of GPS stations. Arrows depict their horizontal velocities with respect to a reference frame fixed on the Somalia Plate. Bold numbers aside the arrows indicate the velocity in mm/yr. Ellipses depict the region of 99% confidence using the uncertainties in Table 1.

about 16 mm/yr and N28°E in azimuth at the southern tip of the Red Sea [DeMets *et al.*, 1994]. Separating Africa into two plates, Somalia and Nubia, Jestin *et al.* [1994] propose a similar relative velocity: 17 mm/yr at azimuth N30°E. Yet the rate of Arabia-Somalia motion varies along the Sheba Ridge from 22 mm/yr at the horn of Africa to 17 mm/yr at the entrance to the Gulf of Tadjoura [DeMets *et al.*, 1994]. For the East African Rift (EAR) that splits Africa into Somalia and Nubia, estimates of the divergence rate also vary considerably: 1 mm/yr [Asfaw *et al.*, 1992], 5 mm/yr [Jestin *et al.*, 1994], or 6 mm/yr [Chu and Gordon, 1999].

[4] In contrast, recent GPS measurements in this area clearly differ from the plate kinematic predictions. Different geodetic studies show that the plate rates consistent with the GPS observations are about 30% slower than the NUVEL-1A estimates for Arabia-Eurasia [McClusky *et al.*, 2000, 2003; Sella *et al.*, 2002; Vernant *et al.*, 2004; Vigny *et al.*, 2006] and Arabia-Somalia [Fernandes *et al.*, 2003; Vigny *et al.*, 2006]. These results suggest that spreading in the Red Sea and the Gulf of Aden, and thus the convergence rate between Arabia and Eurasia, has slowed during the last 3 Ma [Vigny *et al.*, 2006].

[5] At the smaller, regional scale of the Afar Depression, the complexity of the active fault and rift systems leads to

various interpretations. Tectonic observations and paleomagnetic declinations suggest that the Danakil and Ali Sabieh blocks are both rotating [Sichler, 1980; Courtillot *et al.*, 1980; Souriot and Brun, 1992; Manighetti *et al.*, 1998]. The rotations can be understood as a consequence of rift propagation, either as “oceanic microplates” [Acton *et al.*, 1991] or “continental bookshelf faulting” [Tapponnier *et al.*, 1990; Sigmundsson *et al.*, 1992; Manighetti *et al.*, 1998, 2001a, 2001b]. Implicit in all these models is the idea that the deformation transfers from one rift to another and therefore evolves in space and in time. This complication makes evaluating these models by comparing their predictions to quantitative geodetic measurements quite challenging. Confronting long-term, plate-scale models with short-term regional geodetic surveys requires accounting for the dynamics of the underlying processes.

[6] In this paper, we focus on the boundary between the Arabia plate and the Somalia where Sheba Ridge enters into the Afar depression. This narrow, WNW trending zone of active volcanism and tectonics includes Maskali transform fault, the Tadjoura rift and the Asal-Ghoubbet rift. To the NW, it links to the Mak’arassou fault system and the Manda Inakir rift (Figures 1 and 2). The Asal-Ghoubbet rift is

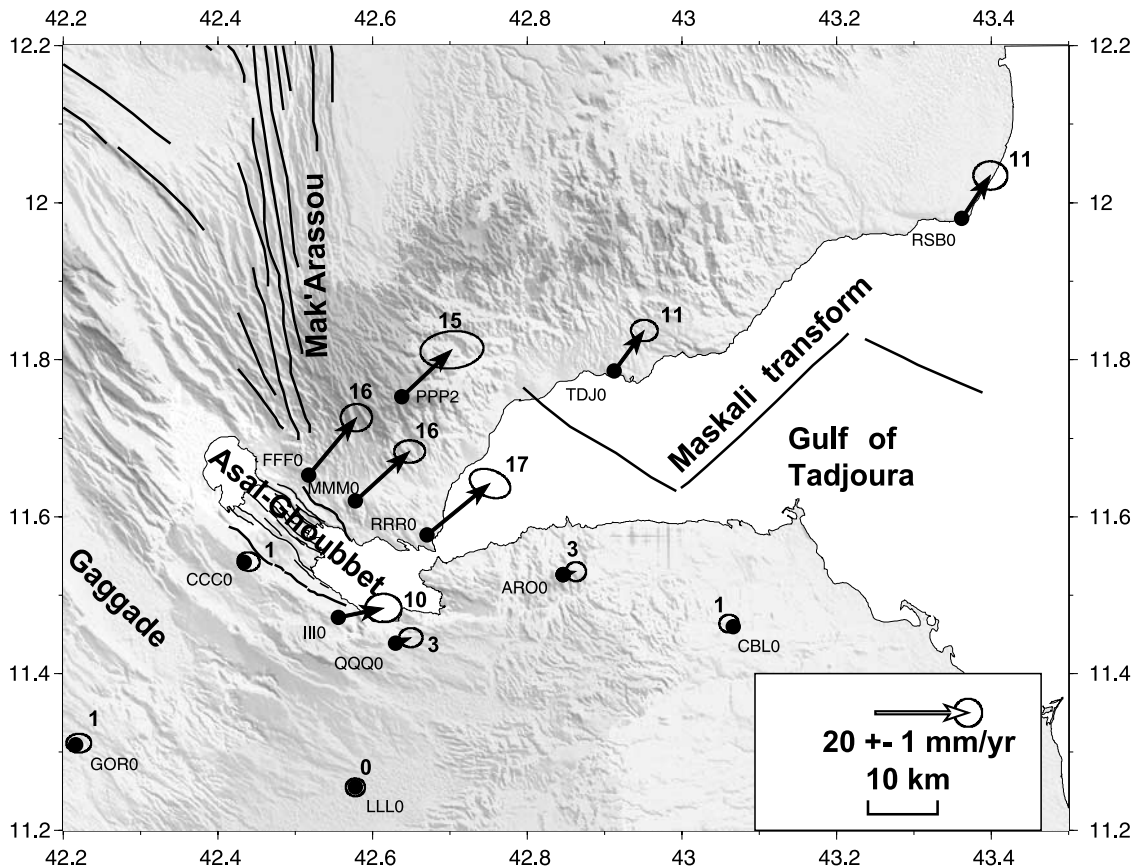


**Figure 2.** Djibouti and Gulf of Tadjoura. Dots show locations of GPS stations. Arrows depict their horizontal velocities with respect to a reference frame fixed on the Somalia plate. Bold numbers beside the arrows indicate the velocity in mm/yr. Ellipses depict the region of 99% confidence using the uncertainties in Table 1. Thick black lines show the principal directions of active rifting (Mak'Arassou, Asal-Ghoubbet, Gulf of Tadjoura) and the Maskali transform fault. Thin gray lines depict faults in the Asal-Ghoubbet rift.

special because we can observe it on dry land to better understand slow spreading ridges in oceanic lithosphere. Reconstructing the edifice of Fieale volcano indicates an average spreading rate of 17 to 29 mm/yr over the last 87,000 to 150,000 years at an azimuth of  $N40^{\circ}E \pm 5$  that is consistent with plate kinematic estimates [de Chabaliier and Avouac, 1994]. The rate of opening at the rift, however, is not constant, as evidenced by a rifting event in 1978. Then, a swarm of earthquakes (two of which had magnitude near 5) reactivated several normal faults, producing a total of 2 m of extension, during a week of volcanic activity at a new eruptive center [e.g., Abdallah et al., 1979]. The geodetic measurements performed during the years following this sequence confirm that strain rates as fast as  $\sim 10^{-6}/\text{yr}$  concentrate in the Asal rift [Ruegg et al., 1979; Ruegg and Kasser, 1987]. All these observations indicate that the Asal-Ghoubbet rift accommodates most of the present-day motion between Arabia and Somalia. Outside the rift, no direct measurements have yet been published to determine which other structure might accommodate any remaining motion.

[7] In this paper we present 12 years of GPS campaign measurements in Djibouti, Yemen, and Ethiopia. At the regional scale, we discuss the strain concentrated in the active rifts spanned by the GPS network. At the local scale, we use over 25 years of geodetic data to argue that transient

rifting episodes like the one in 1978 at Asal are the dominant process in accommodating the motion across this plate boundary. Finally, we confirm this interpretation by considering the vertical displacements measured by GPS and leveling.

## 2. GPS Data Analysis

[8] In November 1991, the first GPS observations were performed in Djibouti and the neighboring parts of Yemen and Ethiopia [Ruegg et al., 1993]. A small subset of this network was surveyed again three times in 1993, once in 1995, and once in 1997 [Walpersdorf et al., 1999]. More complete surveys of the rift network were performed in 1999, 2001, and 2003 (Table S1 in the auxiliary material<sup>1</sup>). The points in Yemen were measured for the second time in 2001, 10 years after the first survey. All sites were measured using a mix of Ashtech and Trimble dual-frequency receivers equipped with different kinds of antennas (see Table S1 for details) During all campaigns, three points (Arta in Djibouti, Sana'a in Yemen, and Addis Abeba in Ethiopia) were measured continuously in 24-hour sessions.

<sup>1</sup>Auxiliary material data sets are available at <ftp://ftp.agu.org/apend/jb/2004/jb003230>. Other auxiliary material files are in the HTML.



**Table 1.** Site Positions and Velocities in ITRF2000 and Relative to Somalia Plate<sup>a</sup>

| Site | Position  |          | Horizontal Velocities |       |         |       | Vertical | Velocity Uncertainties ( $1\sigma$ ) |       |     |             |
|------|-----------|----------|-----------------------|-------|---------|-------|----------|--------------------------------------|-------|-----|-------------|
|      |           |          | ITRF2000              |       | Somalia |       |          | East                                 | North | Up  | Correlation |
|      | Longitude | Latitude | East                  | North | East    | North |          |                                      |       |     |             |
| ARO0 | 42.85     | 11.53    | 33.1                  | 16.2  | 2.7     | 0.7   | -4.8     | 0.7                                  | 0.7   | 0.8 | -0.004      |
| AS00 | 42.46     | 11.64    | 35.5                  | 14.1  | 5.0     | -1.5  | 11.7     | 1.1                                  | 1.0   | 1.4 | 0.000       |
| BY00 | 42.54     | 11.59    | 49.5                  | 25.0  | 13.0    | 9.4   | 2.7      | 1.3                                  | 1.0   | 1.9 | 0.012       |
| CBL0 | 43.07     | 11.46    | 29.4                  | 16.1  | -1.0    | 0.6   | -1.7     | 0.7                                  | 0.6   | 0.9 | 0.001       |
| CCC0 | 42.43     | 11.54    | 31.4                  | 15.8  | 0.9     | 0.2   | 6.1      | 0.8                                  | 0.7   | 1.2 | -0.047      |
| CF00 | 42.49     | 11.62    | 35.1                  | 23.7  | 4.7     | 8.1   | 4.4      | 0.9                                  | 0.7   | 1.2 | 0.012       |
| DF00 | 42.52     | 11.60    | 39.4                  | 24.9  | 9.0     | 9.3   | 7.1      | 0.9                                  | 0.8   | 1.1 | 0.043       |
| EP00 | 42.50     | 11.57    | 35.6                  | 16.2  | 5.2     | 0.6   | 1.4      | 1.0                                  | 0.8   | 1.4 | 0.026       |
| FFF0 | 42.52     | 11.65    | 40.8                  | 28.0  | 10.3    | 12.4  | 10.6     | 1.1                                  | 1.0   | 1.7 | 0.007       |
| FG00 | 42.47     | 11.58    | 30.4                  | 16.6  | -0.1    | 1.0   | 16.5     | 4.0                                  | 1.4   | 5.6 | 0.267       |
| GK00 | 42.47     | 11.60    | 38.5                  | 16.7  | 8.0     | 1.0   | -11.1    | 3.0                                  | 1.1   | 3.5 | -0.086      |
| GM00 | 42.56     | 11.62    | 41.8                  | 25.4  | 11.3    | 9.9   | 5.4      | 0.9                                  | 0.7   | 1.2 | 0.020       |
| GOR0 | 42.22     | 11.31    | 31.1                  | 16.1  | 0.7     | 0.4   | -8.0     | 0.9                                  | 0.7   | 1.7 | 0.002       |
| HD00 | 42.50     | 11.61    | 32.9                  | 18.7  | 2.5     | 3.1   | 1.5      | 1.7                                  | 1.5   | 3.4 | 0.007       |
| HM00 | 42.50     | 11.55    | 36.9                  | 16.5  | 6.5     | 0.8   | 19.0     | 4.6                                  | 2.2   | 8.4 | 0.168       |
| HX00 | 42.43     | 11.59    | 36.3                  | 19.6  | 5.9     | 3.9   | 5.0      | 1.3                                  | 1.0   | 2.3 | 0.021       |
| III0 | 42.56     | 11.47    | 40.1                  | 17.6  | 9.7     | 2.0   | 6.8      | 1.3                                  | 1.0   | 2.1 | 0.003       |
| LLL0 | 42.58     | 11.26    | 30.3                  | 15.6  | -0.4    | -0.2  | -2.0     | 0.7                                  | 0.6   | 0.9 | -0.002      |
| LS00 | 42.52     | 11.57    | 36.7                  | 15.6  | 6.3     | 0.0   | -2.1     | 0.9                                  | 0.7   | 1.5 | 0.020       |
| MMM0 | 42.58     | 11.62    | 42.1                  | 26.3  | 10.7    | 10.7  | 6.9      | 1.1                                  | 0.8   | 2.2 | 0.009       |
| PPP2 | 42.64     | 11.75    | 41.3                  | 25.6  | 10.8    | 10.1  | 1.3      | 2.2                                  | 1.3   | 5.4 | 0.098       |
| QQQ0 | 42.63     | 11.44    | 33.7                  | 16.7  | 3.2     | 1.2   | 1.9      | 0.8                                  | 0.7   | 1.4 | 0.008       |
| RRR0 | 42.67     | 11.58    | 43.9                  | 26.6  | 13.5    | 11.1  | 3.3      | 1.4                                  | 1.0   | 2.8 | -0.308      |
| RSB0 | 43.36     | 11.98    | 36.7                  | 24.6  | 6.1     | 9.3   | 0.8      | 0.8                                  | 0.7   | 1.8 | -0.010      |
| SAD0 | 42.69     | 11.61    | 39.1                  | 19.8  | 8.6     | 4.3   | 9.5      | 2.2                                  | 1.5   | 4.4 | 0.021       |
| SN00 | 42.52     | 11.59    | 39.1                  | 16.4  | 8.7     | 0.8   | 4.0      | 1.5                                  | 1.1   | 3.2 | 0.079       |
| TDJ0 | 42.91     | 11.79    | 36.9                  | 24.2  | 6.4     | 8.7   | -2.1     | 0.9                                  | 0.8   | 1.4 | -0.024      |
| ADD1 | 38.77     | 9.04     | 25.3                  | 16.5  | -4.4    | -0.3  | -0.5     | 0.7                                  | 0.7   | 0.8 | 0.002       |
| DHAM | 44.39     | 14.58    | 35.6                  | 28.0  | 4.4     | 13.0  | -1.9     | 0.8                                  | 0.7   | 1.3 | -0.016      |
| HODD | 42.97     | 14.79    | 35.3                  | 26.8  | 4.2     | 11.3  | -4.5     | 1.0                                  | 0.8   | 1.9 | -0.053      |
| JNAR | 43.44     | 13.32    | 37.2                  | 26.7  | 6.3     | 11.4  | -5.7     | 1.3                                  | 0.8   | 2.9 | -0.067      |
| SANA | 44.19     | 15.35    | 37.0                  | 26.5  | 5.6     | 11.4  | -1.1     | 0.8                                  | 0.7   | 0.9 | -0.013      |

<sup>a</sup>Latitude and longitude are in decimal degrees. All velocities and velocity uncertainties are in mm/yr.

Other sites in Djibouti were measured for 6 to 24 hours per day over 1 to 6 days (Table S1).

[9] We reduce these data in 24-hour sessions to daily estimates of station positions using the GAMIT software [King and Bock, 2000], choosing the ionosphere-free combination, and fixing the ambiguities to integer values. We use precise orbits from the International GPS Service for Geodynamics (IGS) [Beutler et al., 1993]. We also use IGS tables to describe the phase centers of the antennae. We estimate one tropospheric delay parameter per station every 3 hours. The horizontal components of the calculated relative position vectors are precise to within a few millimeters for pairs of stations less than 150 km apart, as measured by the root mean square (RMS) scatter about the mean.

[10] In the second step, we combine the daily solutions using the GLOBK software [Herring et al., 1990] in a “regional stabilization” approach [McClusky et al., 2000]. To define a consistent reference frame for all epochs, we include tracking data from the permanent stations of the International GPS Service (IGS) [Neilan, 1995]. The number of IGS stations around our study area available at the time of our campaigns was 4 in 1991 but increased to 42 in 2003. These fiducial stations are also included in the daily global GAMIT solutions from the IGS data center at Scripps, including more than 200 stations spread all over the globe. We combine all these daily solutions using

Helmert-like transformations to estimate translation, rotation, scale and Earth orientation parameters (polar motion and UT1 rotation). This “stabilization” procedure defines a reference frame by minimizing, in the least squares sense, the departure from the prior values determined in the International Terrestrial Reference Frame (ITRF) 2000 [Altamimi et al., 2002]. This procedure estimates the positions and velocities for a set of 22 well-determined stations in and around our study area. The misfit to these “stabilized” stations is 2.8 mm in position and 1.6 mm/yr in velocity. More details about this solution and velocity residuals are given by Vigny et al. [2006].

### 3. Horizontal Velocities

[11] This procedure leads to horizontal velocities with respect to ITRF2000 (Table 1). We compute velocities relative to the Somalian plate by using the angular velocity of this plate ( $48.12^\circ\text{N}$ ,  $-97.75^\circ\text{W}$ ,  $0.329^\circ/\text{Ma}$ ) given by Vigny et al. [2006]. In this reference frame, three sites in southern Djibouti (CBL0, LLL0, GOR0) located far from the rift axis and supposedly on the Somalian plate, show velocities smaller than 1 mm/yr (Figures 1 and 2 and Table 1). Three more stations immediately south of the Asal-Tadjoura rifts (ARO0, QQQ0, and CCC0) also exhibit little motion, whereas site III0 is a notable exception (Figure 2 and Table 1). Therefore we chose to show all velocities in this

reference frame, i.e., with respect to the Somalia plate. This choice has the advantage of highlighting the deformation in and around the Asal rift because the velocities of sites on the stable area south of it appear as short, insignificant arrows.

### 3.1. Far-Field Velocities

[12] In this Somalia-fixed reference frame, the residual velocity in Addis Abeba (ADD1), west of the East African Rift (EAR), is 4 mm/yr ( $\pm 1$  mm/yr at  $1\sigma$ ), oriented roughly west (Figure 1 and Table 1). The amplitude of this residual vector depends on the angular velocity estimated for the Somalia plate. Different solutions give velocities between 3 and 6 mm/yr that are consistent within 95% confidence. Their azimuths fall between west and northwest, roughly perpendicular to the EAR trace at this latitude. Therefore we conclude that our value of 4 mm/yr  $\pm 2$  is an upper bound for the EAR opening rate just south of the Afar depression.

[13] The stations in Yemen (DHAM, HODD, JNAR, SANA) move together as a coherent block that represents a part of the Arabia plate with very little internal deformation (Figure 1). The azimuth of their average velocity ( $N25^\circ \pm 5$ ) is compatible with the orientations of Gulf of Aden transform faults used to determine the NUVEL-1 model [DeMets *et al.*, 1990]. On the contrary, their mean opening rate ( $13 \pm 2$  mm/yr) is 30% slower than the Nuvel-1A rate [Vigny *et al.*, 2006]. This definition of the Arabia plate implies that two stations located at the southern tip of the Danakil block (TDJ0 and RSB0) are close to having “Arabian” velocities (Figure 1). Their residual motion with respect to the four stations in Yemen is less than 2 mm/yr. This result confirms that the opening rate of the Red Sea at this latitude is negligible, which is not surprising given the absence of magnetic anomalies on the seafloor there. Therefore we conclude that most, and possibly all, of the present-day opening is accommodated west of the “Danakil block” represented by RSB0 and TDJ0 (Figure 1).

[14] With respect to the African plate defined by Vigny *et al.* [2006] ( $50.48^\circ N$ ,  $-82.01^\circ E$ ,  $0.265^\circ Ma$ ), the motion of these two points (RSB0 and TDJ0) is  $15 \pm 2$  mm/yr at  $N54 \pm 6^\circ$ . Assuming that the Danakil block rotates about a pole near its northern end (at  $16^\circ N$ ,  $40^\circ E$ ), we find an angular velocity of  $1.6 \pm 0.1^\circ Ma$  for the Danakil block. This spin rate agrees with the paleomagnetic estimate of  $10.7^\circ \pm 4^\circ$  over 7 Ma, which gives an average rate of  $1.5 \pm 0.6^\circ Ma$  or  $26 \pm 10 \mu rad/yr$  [Manighetti *et al.*, 2001a; Besse and Courtillot, 1991]. Therefore we conclude that the spreading between Arabia and Africa at this latitude has been taking place west of the “Danakil block”, i.e., along the deformation zones of the Afar depression, for at least the last 7 Ma.

### 3.2. Djibouti and the Gulf of Tadjoura

[15] Deformation along the northern side of the Gulf of Tadjoura (Figure 2) exhibits a clear gradient from 16 mm/yr on the northeastern Asal-Ghoubbet rift shoulder to 11 mm/yr in the Danakil block (RSB0, TDJ0). Stations FFF0, MMM0, and RRR0, lying at the same distance from the Asal-Ghoubbet rift axis, display a coherent velocity of  $16 \pm 1$  mm/yr and  $N45^\circ \pm 8^\circ$  on average. We are particularly confident in the velocity of point FFF0 since it has been measured four times during the last 12 years with a remarkably stable time series. Point PPP0, located at intermediate distance between the “Danakil-Arabian” area and

the rift shoulder, has a transitional velocity of  $15 \pm 3$  mm/yr with the same azimuth.

[16] On the southwestern side of the Asal-Ghoubbet rift, we observe no significant velocity gradient between the southern rift shoulder (CCC0 or QQQ0) and the Somalia plate as we have defined it. Yet this interpretation is subject to two caveats: First, there are no GPS sites between GORO in the far field and the southern rift shoulder. Second, the motions of QQQ0 and III0 differ markedly: the former has a small insignificant residual velocity, while the latter has an unexpected and probably erroneous high velocity of 10 mm/yr. Despite these caveats, we infer an asymmetry in the extensional deformation pattern between the northern part and the southern part of the Asal-Ghoubbet rift. This asymmetry is also apparent in the vertical deformation recorded by the topography, the faults activated during the 1978 sequence, and the way individual faults shift their activity to the northeast [Ruegg *et al.*, 1990; Stein *et al.*, 1991; Ruegg and Kasser, 1987].

[17] All these results confirm that Asal-Ghoubbet rift accommodates most of (indeed, more than) the present-day motion of Arabia-Somalia expected during the 12-year observation period. In particular, the dense GPS network along the coast of the Gulf of Tadjoura shows no measurable deformation, either within the Tadjoura rift or on the faults between the Tadjoura and Asal rifts. Nor do we see any evidence for slip or creep on the active Gaggade-Hanle fault system, southwest of the Asal rift. Accordingly, we infer that the faults there are locked during this time interval.

[18] Why, then, is the extension rate of 16 mm/yr across the Asal rift some 50% faster than the Arabia-Somalia plate motion? The most probable explanation involves the transient processes that took place in the rift following the 1978 seismovolcanic sequence, when up to 1.9 m of extension were measured across the rift [Ruegg *et al.*, 1979]. During the following decade, extension at a rate of 60 mm/yr has been measured across the inner rift fault system that was activated during the 1978 sequence [Ruegg and Kasser, 1987]. After 1987, this rate decreased to about 1 cm/yr, slower than the far-field rate imposed by large-scale plate tectonics (Figure 3). That the rate of opening changed drastically in the 6 years following the 1978 rifting event suggests two possible interpretations.

[19] In the first interpretation, the opening continued at a constant rate of 53 mm/yr from 1980 through 1986 [Ruegg and Kasser, 1987]. Then the rate of opening slowed abruptly to 13 mm/yr, close to the geologic plate rate, suggesting that driving processes ceased abruptly. Although this model, with three parameters (two slopes and an intercept), is the simplest possible description of the time series shown in Figure 3, it does not appear to be compatible with other geophysical observations. In particular, there is no suggestion of a similar change in the seismicity around 1986. Nor do field observations suggest that the seismovolcanic activity that “boiled over” in the 1978 crisis continued to simmer for the next 8 years. Fresh lava, for example, was observed only in 1978.

[20] The second interpretation involves postseismic relaxation in the years following the 1978 rifting event. One simple model for this is a one-dimensional Elsasser formulation, consisting of an elastic layer over a viscous layer, as

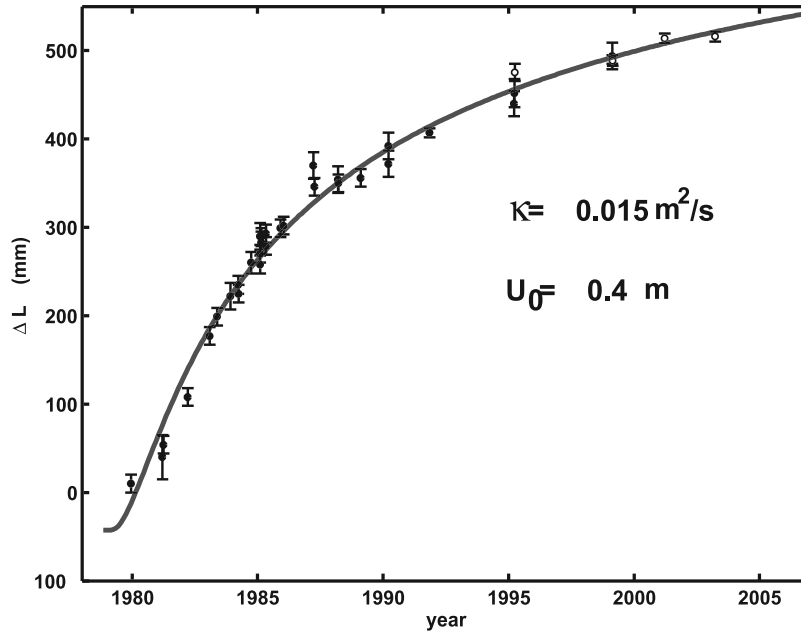


**Figure 3.** Time-dependent opening of the rift following the 1978 rifting event. The dots show the distance between stations EP00 and DF00 on opposite sides of the rift (see Figure 4 for location). Solid symbols depict range measurements. Open symbols denote GPS measurements (since 1995). The vertical bars show one standard deviation for each measurement. Line is the best fitting curve calculated from the diffusive elastic-over-viscous model (1).

suggested for a similar rifting event in 1974 at Krafla, Iceland [Foulger *et al.*, 1992; Sigmundsson, 2006]. The upper, elastic layer has thickness  $h$  and rigidity  $\mu$ . The lower, viscous layer has Newtonian dynamic viscosity  $\eta$  and thickness  $b$ . This configuration of geometry and rheology leads to the diffusion equation with a stress diffusivity  $\kappa$ . Accordingly, the pulse of stress produced by the initial dike injection diffuses away from the axis. For a dike of half width  $U_0$ , intruded into the elastic layer at time  $t = 0$ , the resulting horizontal displacement is

$$u(x, t) = U_0 \operatorname{erfc} \frac{x}{2\sqrt{\kappa t}} \quad (1)$$

where  $x$  is the distance from the rift, and  $\operatorname{erfc}$  is the complementary error function [Foulger *et al.*, 1992]. Fitting the geodetically observed values in Figure 3, we find an initial half opening of  $U_0 = 0.4$  m and a stress diffusivity of  $\kappa = 0.015$  m<sup>2</sup>/s. The value of the full initial opening  $2U_0$  estimated from fitting the data is about half of the 1.9 m of opening measured in 1978 [Abdallah *et al.*, 1979]. The stress diffusivity  $\kappa$  may be interpreted as the product of the two thicknesses divided by a timescale  $\tau$ :

$$\kappa = \frac{hb}{\tau} \quad (2)$$

In the case of a Poisson solid with a Poisson ratio of  $1/4$ , the timescale  $\tau$  is proportional to the ratio of the viscous effects to the elastic effects:

$$\tau = \frac{3\eta}{8\mu} \quad (3)$$

[21] Having established that velocities in the area change with time, one might worry that velocities inferred from campaign GPS measurements represent only an average on the time interval between two epoch measurements. In this case, comparing measurements made at different epochs at different locations might cause aliasing. However, time series of the distance across the rift axis from EP00 DF00 shows an approximately constant rate between 1987 and 2003 (Figure 3). In other words, the transient has decayed sufficiently so that it can be fit reasonably well by a constant linear rate for the time span of our GPS campaigns (1991–2003). The misfit is less than 2 mm/yr, consistent with the uncertainties in the GPS velocity estimates.

### 3.3. Asal Rift

[22] Figure 4 shows the details of the deformation field inside the Asal rift, as measured by the relative velocities of about 20 points throughout the rift valley (Figure 4). As at the larger scale, the rate of opening observed on the NE shoulder of the Asal rift is very coherent, with a constant rate of 16 mm/yr  $\pm 1$  at azimuth  $N45^\circ \pm 8^\circ$  for the line through stations FFF0, GM00, MMM0, and RRR0. These stations move together as a unit that we call a “panel” that can be defined by the geomorphic expression of the active faults bounding it.

[23] Nearer the rift axis, on the next panel to the southwest, we observe a marked variation along the strike of the panel: 16 mm/yr at BY00, 13 mm/yr at DF00, 10 mm/yr at CF00 and 6 mm/yr at AS00. This last line of points is located at the northern border of the “Petit Rift”, a rift-in-rift structure with a dense network of faults, open fissures, and cracks that appears to be the most active part of the Asal rift. The line formed by these benchmarks also

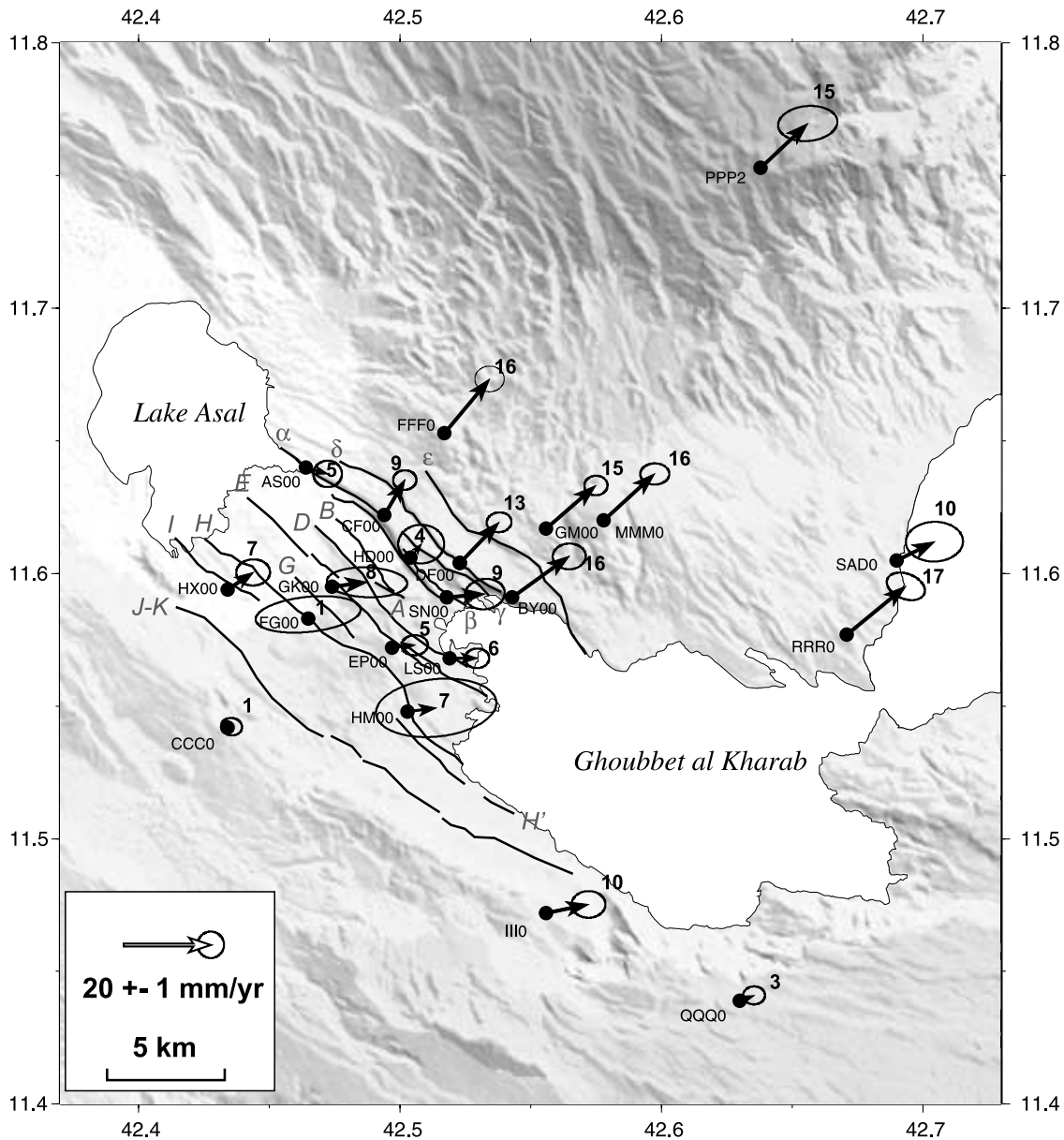


**Figure 4.** Asal rift. Dots show locations of GPS stations. Arrows depict their horizontal velocities with respect to a reference frame fixed on the Somalia plate. Bold numbers aside the arrows indicate the velocity in mm/yr. Ellipses depict the region of 99% confidence using the uncertainties in Table 1. Lines show the main active faults in the Asal rift.

describes the northern boundary of the set of faults that slipped during the 1978 seismovolcanic sequence. The GPS stations' velocities decrease from SE to NW, following the shape of the Petit Rift that terminates just southeast of station CF00 [de Chabaliere and Avouac, 1994]. This rate variation indicates propagation from SE to NW, as suggested from geomorphologic observations [Manighetti et al., 1998]. This propagation appears to be shallow, probably less than 3–4 km deep, because its effects do not reach the previous panel: FFF0, GM00, MMM0, and RRR0 move with the same velocity.

[24] On the southwestern side of the rift, the velocity field is not so clear, mainly because stations (HM00, FG00, GK00, and HX00) have large uncertainties that reflect

infrequent measurements. Nonetheless, we can define a shoulder panel including the stations HX00, FG00, and HM00 with speeds of 1 to 7 mm/yr, and another panel including stations GK00, EP00, and LS00 with a velocity of about 5–8 mm/yr. Points HD00 and SN00, located close to the rift axis, show rates of 4 and 9 mm/yr with respect to the Somalian plate, respectively. The general pattern on the southwest side of the rift indicates a small, gradual increase in velocity from the southwestern shoulder to the axis.

[25] To visualize the high strain rates concentrated in the Asal rift, we project the velocities onto four profiles striking 45°E, perpendicular to the rift axis (Figure 5). The average strain rate is 1 mm/yr/km (or  $3 \times 10^{-14} \text{ s}^{-1}$ ). Most of the points on the NE side of the rift axis move faster than this



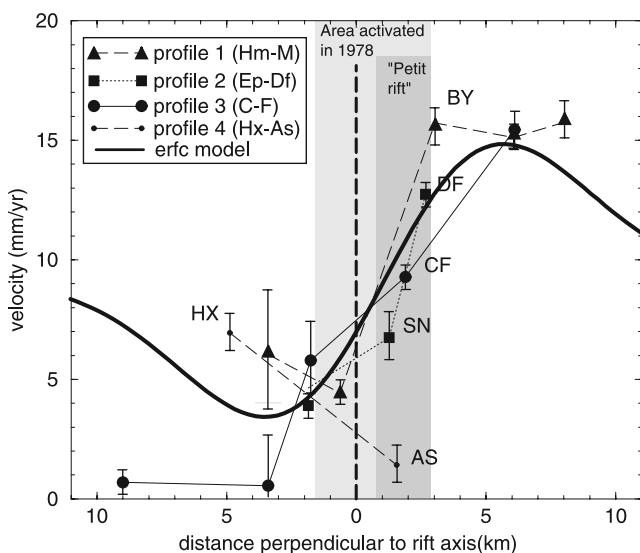


**Figure 5.** Horizontal velocity components for stations in the Asal rift plotted along profiles perpendicular to the rift axis. The thick dashed line shows the rift axis. Rectangular shaded areas indicate the extents of the 1978 rifting event (light) and the Petit Rift (dark). The thick black curve depicts the erfc elastic-over-viscous model computed with the parameters inferred from model curve in Figure 3 and  $t = 19$  years since 1978 and centered at +1 km. Triangles and dashed line depict the first profile near Ghoubbet (HM00 – LS00 – BY00 – GM00 – MMM0). Squares and dotted line depict the second profile (EP00 – SN00 – DF00). Circles and solid line depict the third profile near lake Asal (CCC0 – FG00 – GK00 – CF00 – FFF0). Dots and long dashed line depict the last two points at lake Asal (HX00 – AS00). Error bars represent the 1-sigma uncertainties of Table 1.

average strain rate, while those in the SW part move more slowly. This signature becomes clearer if we neglect stations HX00 and AS00 (profile 4) that sit near Lake Asal and are therefore perturbed by the along-strike variation due to the northwestward propagation of the rift. Indeed, this signature is expected from the diffusive model. The curve in Figure 5 shows the velocity calculated using the one-dimensional Elsasser model [Foulger *et al.*, 1992, equation 4] with the diffusivity  $\kappa$  and initial opening  $U_0$  estimated above, an elapsed time of 19 years between the crisis in 1978 and the mean date [1997] of our GPS campaigns, and located at a distance of  $x = 1$  km northeast of the main rift axis. The deformation concentrates to the NE of the geomorphologic long-term rift axis such that the highest velocity gradient occurs in the Petit Rift between stations SN00 and DF00–BY00 (Figure 5). This area coincides with the maximum of fault breaks observed during the 1978 sequence [Le Dain *et al.*, 1979; Ruegg *et al.*, 1979] and with the present-day seismicity, which is mostly located in the northern part of the rift [Doubre *et al.*, 2005]. Furthermore, the fastest points, showing the location of the postseismic diffusive pulse in 1997, fall 3 to 5 km away from the Petit Rift axis on the northeast side. However, the major limitation of this simple model lies in its symmetry with respect to the rift axis, which causes a large misfit at station CCC0 on the southwest side. Therefore we conclude that this model is a reasonable a first-

order approximation. A more sophisticated, second-order approximation should account for geometric complexities such as creep on dipping faults.

#### 4. Rates of Vertical Motion

[26] Conditions in the Asal rift are good for measuring the vertical component of the tectonic deformation field. Some points of our network have been measured many times over a 12-year interval. Measurement campaigns were usually conducted at the same time of the year, during winter. Relative distances between points are small. Finally, almost all points are located on good, solid outcrops, clearly attached to the bedrock. The floor of the innermost valley in the rift could be subsiding as fast as 10 mm/yr with respect to the shoulders. Accordingly, we expect the ratio of tectonic signal to geodetic measurement uncertainty to be larger than unity.

##### 4.1. Intermediate-Scale GPS

[27] Selecting stations measured at least four times, we define a subset of points around the rift with vertical velocities determined to within  $\pm 5$  mm/yr (Figure 6). Stations located far from the rift (RSB0 and TDJ0 on the north side and CBL0 and LLL0 on the south side) show no motion to within  $\pm 2$ –3 mm/yr. They represent a stable reference frame for analyzing vertical motions in the rift. Near the eastern tip of the rift, stations RRR0 and QQQ0 also show small, but marginally significant, velocities of +2 to +3 mm/yr upward with respect to the far-field reference. Points located further west on the shoulders of the rift show a fairly symmetric and significant uplift between 6 and 11 mm/yr. From these values, we can estimate an average uplift value of  $8 \pm 3$  mm/yr and locate the maximum uplift in the central part of the rift, midway between Lake Asal and Ghoubbet Al Kharab.

##### 4.2. Small Scale: Leveling and GPS Inside the Rift

[28] To measure vertical motions over short distances, classical spirit leveling is usually more appropriate than GPS. With care, one can limit the drift of the technique to less than one part per million (1 mm per km). It is therefore possible to detect millimeter-sized vertical displacements between two leveling surveys made on the same line at different epochs. A precise leveling line with about 200 marks was established in 1973 along 100 km of the road crossing the rift. The central part of this line was measured for the second time in 1979, after the Ardoukoba seismic-volcanic crisis [Abdallah *et al.*, 1979; Ruegg *et al.*, 1979], and again in the winter of 1984–1985 [Ruegg and Kasser, 1987]. Over this 6-year interval, uplift rates as fast as 10 to 15 mm/yr were detected. The pattern is similar on both sides of the rift axis. The inner floor subsides with respect to the shoulders, but uplifts with respect to the far field.

[29] This leveling line was measured for the fourth time in 2000. The 1985–2000 comparison gives vertical rates over a 15-year period (Figure 7). The inferred pattern of deformation shows both similarities and differences with the 1978–1985 one. Both intervals show the same pattern of uplift of the rift shoulders and relative subsidence of the inner floor. Yet the rates for the 1985–2000 interval are 50% slower than those for 1978–1985, indicating that the postseismic transient after the 1978 crisis is still decaying.

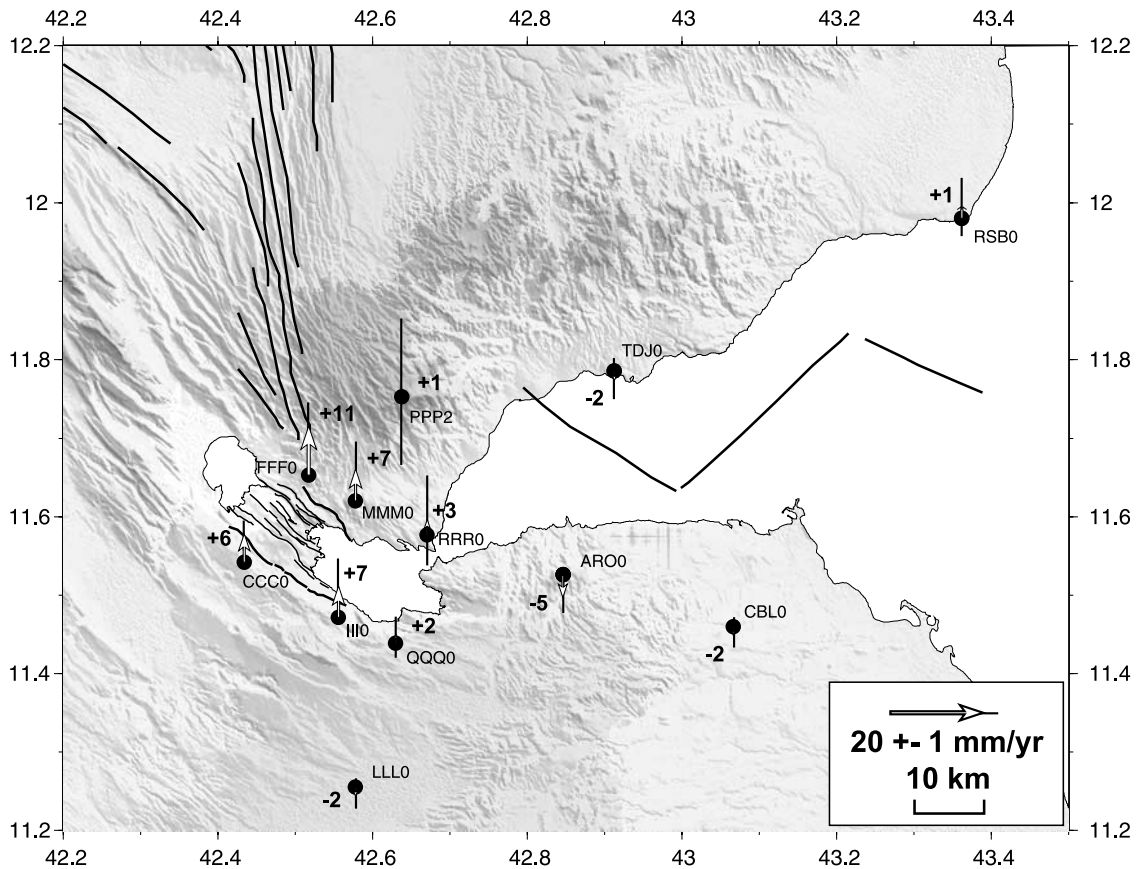


**Figure 6.** Vertical velocities in Djibouti. Dots show locations of GPS stations measured at least 3 times. Arrows depict the GPS vertical velocities at those locations: arrows pointing north indicate upward velocities. Numbers beside the arrow heads indicate the velocities in mm/yr. Vertical thin lines at the arrow heads give the 99% confidence level using uncertainties from Table 1.

The peak around km 32 in the inner rift floor appears to represent the same two-dimensional effect as seen in the horizontal velocities. Since this portion of the leveling line runs parallel to the rift axis, the uplift varies as a function of position along strike, probably reflecting the same propagation process. The points on the NE side (after km 45) differ from previous measurements. They suggest that the uplifting area was wider after 1985 than before, consistent with the diffusive Elsasser model.

[30] This finding is consistent with recent INSAR results obtained for the 1997–2003 interval [Dobre et al., 2005]. Yet this finding should be taken with some caution. Systematic errors in the leveling measurements could conceivably produce a systematic pattern. The change in height at the end of the line is only 75 mm with respect to the starting point 65 km away. The overall trend is only slightly more than 1 mm/km, close to the measurement uncertainty. Unfortunately, the line was measured in a forward run only, preventing us from using the misclosure to estimate the uncertainty. Also, the measurements stopped short of the end point of the 1973 line in the far field. Consequently, we must rely on the internal error analysis to evaluate the precision of this leveling profile. The lines of sight were kept short: 15 m on average and very seldom longer than 30 m (Figure S1a in the auxiliary material). Forward and backward lines of sight were symmetric within 10 to 20% to

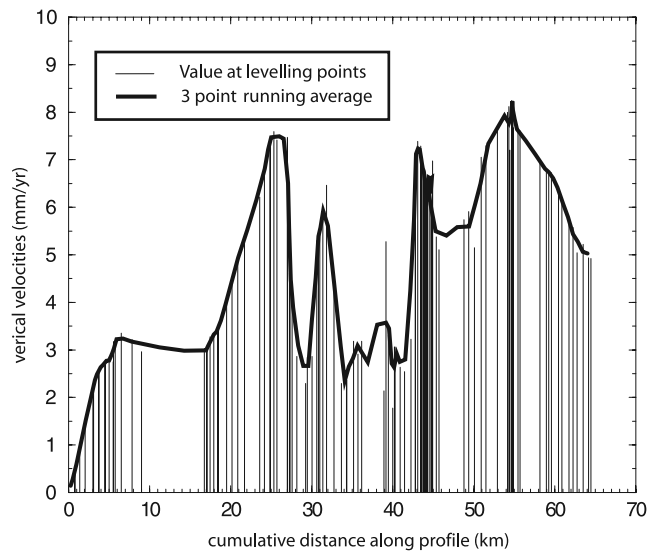


**Figure 7.** Leveling profile velocities (2000–1985) projected on an axis perpendicular to the rift (strait grey line on Figure 8). The vertical thin lines indicate the difference between 2000 and 1985 measurement at each bench mark of the profile. The thick curve is a three-point running average of these measurements.

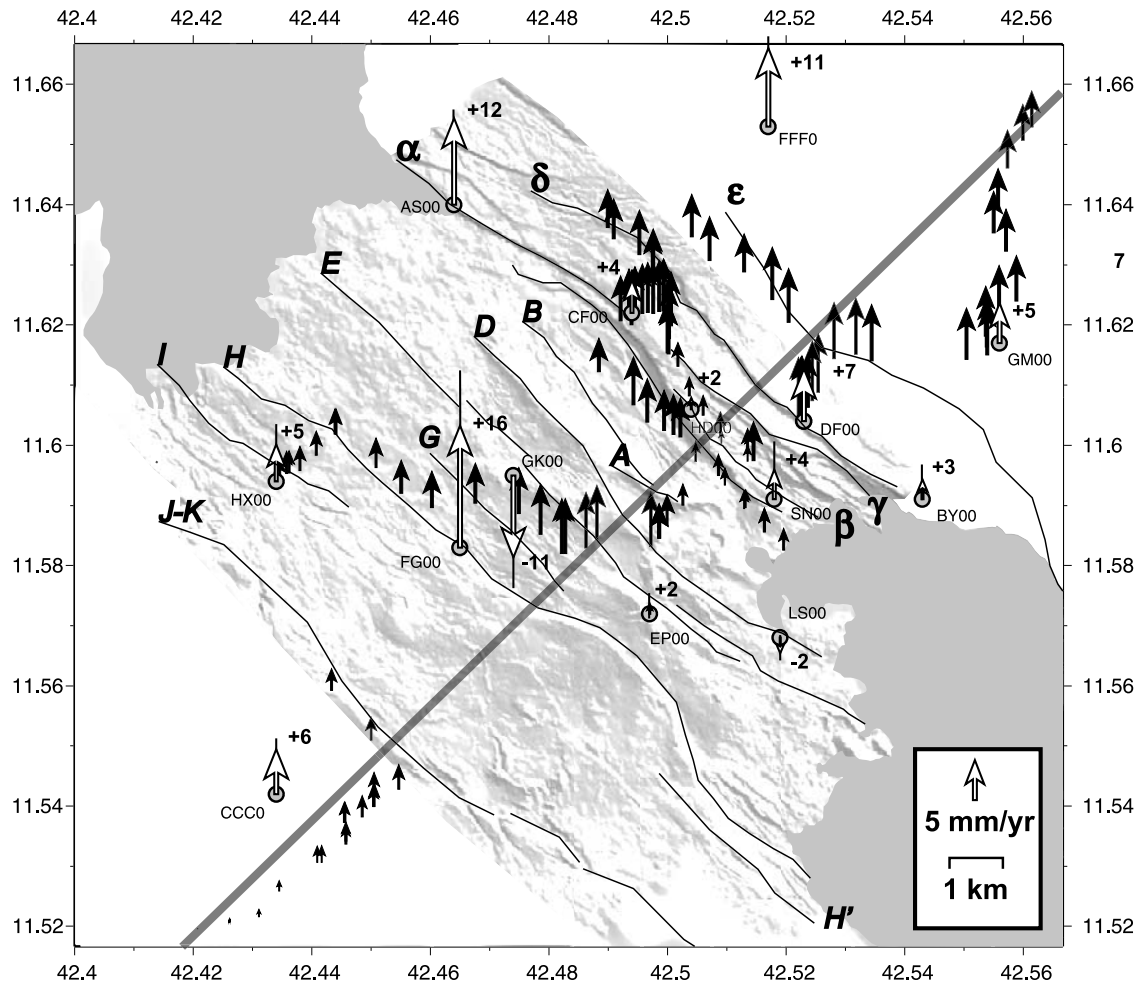


**Figure 8.** Vertical velocities inside the Asal rift. Dots show locations of GPS stations. Open arrows depict the GPS vertical velocities. Solid arrows depict the velocities obtained from leveling profiles. Arrows pointing north indicate upward velocities. Vertical thin lines at the arrow heads give the 99% confidence level using Table 1 vertical velocity uncertainty (no uncertainties for the leveling velocities). Bold numbers aside the arrowheads indicate the velocity in mm/yr. Gray line shows the direction along which the one-dimensional profile of Figure 7 is plotted. The background topography is from the 10 m resolution digital elevation model made from aerial photography [de Chabaliere and Avouac, 1994]. Fault labels (A-K and  $\alpha-\epsilon$ ) are from Stein et al. [1991].

cancel out any asymmetric behavior of the leveling instrument (Figure S1b). We avoided as much as possible hitting the surveyor's pole at low heights, near the ground where atmospheric distortions are largest (Figure S1c). Finally, the 10 small loops of length shorter than 1 km all closed to within 1 mm, without any systematic trend (Figure S1d). Considering all these reasons together, we can exclude systematic errors as the cause of the uplift observed on the northeast side of the rift.

[31] However, a change of height does not necessarily imply a change of topographic elevation. It could be that the local geoid changed over the 15-year time span between the two leveling surveys. Indeed, some indication that this may have occurred comes from gravity measurements conducted in the area in 1999 [Ballu et al., 2003]. These measurements suggest that the gravitational acceleration decreased in this area between 1985 and 1999. Such a change could be interpreted in terms of uplifting the benchmarks, decreasing

the density of the rocks below them, or some combination of the two.

[32] We can glean a little more information from a two-dimensional comparison with the vertical velocities for the GPS stations inside the rift. Again selecting stations measured at least four times, we see some coherent signal (Figure 8). The results are similar if we select three occupations over a minimum of eight years. First, this map view highlights the two-dimensional distribution of the vertical motions. Far from being a straight line across the rift, the leveling line meanders around faults and cliffs and samples the uplift at different locations along the rift axis. Thus the signal on the rift inner floor varies along its strike: less than 1 mm/yr near the Ghoubbet shore but close to 5 mm/yr some 5 km inland. Second, there is a general agreement between the GPS and leveling estimates on the NE side of the rift. Both techniques see the shoulder uplifting at 5 to 7 mm/yr (GM00 and DF00). The next



panel, represented by station CF00, is rising by only 4 mm/yr with respect to the valley floor, but subsiding with respect to the shoulder. The inner rift floor is clearly subsiding, with 2 to 4 mm/yr in the Petit Rift (stations HD00 and SN00). Points on the other side of the rift axis, but close to the Ghoubbet have very small velocities (+2 mm/yr at EP00, -2 mm/yr at LS00). All these values are consistent with the leveling values, except GK00 and FG00 which have large uncertainties. They indicate the sum of two signals: a subsidence of the inner floor with respect to the shoulders and an inflation signal located in the middle of the rift. The SW side of the rift is different: GPS vectors indicate an uplift of the rift shoulder where the leveling shows none (HX00 and CCC0).

## 5. Conclusion

[33] *Vigny et al.* [2006] have shown that the far-field plate rates estimated from GPS data acquired over the 12-year interval are 30% slower than predicted by plate motion models based on the last several million years. Our estimate for the rate of opening across the Asal rift between Somalia and the Danakil block is  $11 \pm 1$  mm/yr, based on 10 GPS stations observed between 1991 and 2003. Clearly, the deformation pattern across this complex plate boundary is more complicated than supposed by classical plate tectonics, which neglects internal deformation within each plate.

[34] The rifting event in 1978 created a significant transient in the deformation pattern. Over 25 years later, the inner rift is still opening at a rate faster than the far-field value. This observation can be mimicked to first order by a simple one-dimensional Elsassner model of an elastic layer over a viscous layer. For the 1978 Asal crisis in Djibouti, however, the estimated diffusivity is 2 orders of magnitude smaller than estimated for the 1974 Krafla crisis in Iceland [*Foulger et al.*, 1992]. The diffusivity measures the ratio of the product of the two thicknesses (or length scales) to the timescale. The timescale is the time between the rifting episode and the second geodetic survey, i.e., 19 years at Asal and 11 years at Krafla. One length scale is the distance from the rift axis to the fastest moving point (at that time), 3 km at Asal, considerably shorter than the 25 km at Krafla. The diffusivity ratio for Asal with respect to Krafla is  $\sim 1/70$ , implying that the top elastic layer is at least an order of magnitude thinner beneath Asal and/or that the viscosity of the underlying substrate is at least an order of magnitude higher at Asal than at Krafla. Although these differences are qualitatively consistent with the tectonic settings of Djibouti and Iceland, their stark quantitative contrast suggests that the one-dimensional analysis oversimplifies the problem somewhat.

[35] *Cattin et al.* [2005] show that a sophisticated model can fit the data better. For example, geometric considerations (multiple dipping, nonplanar faults) and thermal effects (postrifting cooling increases viscosity) lead to a complete three-dimensional approach using numerical modeling. Such a model can explain the details of the inner rift deformation. For example, the geodetic data shown here suggest that the northern part of the rift zone accommodates more (some 70%) of the extension than the southern part.

[36] Considering the amount of extension absorbed in the Asal rift during the 1978 sequence, the high postseismic

velocity, and the present-day velocity, we infer that the opening rate across the Asal rift will have to decrease significantly before the next such seismovolcanic crisis can occur. The deformation recorded by the topography as well as the deformation recorded by the lake Asal Holocene markers, suggest that the recurrence time of such a crisis is about 120 to 300 yr [*Ruegg et al.*, 1990; *Stein et al.*, 1991; *Manighetti et al.*, 1998]. However, the ongoing high rate and the fact that the rift and the flanks are both rising as a whole with respect to the far-field plate interiors are two indications that magma injection still prevails over extension as the active process driving the rifting today.

[37] **Acknowledgments.** We are grateful to many people who participated in measurement campaigns, especially individuals from the "Observatoire d'Arta." We thank J.-C. Delmont, who was its director during the 1991 campaign and participated in the 1995 and 1999 campaigns. The leveling line was surveyed by A. Coulomb from IGN. Very special thanks to Moumin in Djibouti. The Afar geodetic program was sponsored by CNRS/INSU programs (Tectoscope-Positionnement, IDHYL, IT). We also appreciate the guidance of Peter Molnar, who read the manuscript twice and obtained a grant from NSF (OCE8916680) that boosted the 1991 campaign.

## References

- Abdallah, A., et al. (1979), Relevance of afar seismicity and volcanism to the mechanics of accreting plate boundaries, *Nature*, 282, 17–23.
- Acton, G. D., S. Stein, and J. F. Engeln (1991), Block rotation and continental extension in Afar: A comparison to oceanic microplate systems, *Tectonics*, 10, 501–526.
- Altamimi, Z., P. Sillard, and C. Boucher (2002), ITRF2000: A new release of the International Terrestrial Reference Frame for earth science applications, *J. Geophys. Res.*, 107(B10), 2214, doi:10.1029/2001JB000561.
- Asfaw, L. M., et al. (1992), Recent inactivity in African rift, *Nature*, 357, 447.
- Ballu, V., et al. (2003), 1985–1999 gravity field variations across the Asal rift: Insights on vertical movements and mass transfer, *Earth Planet. Sci. Lett.*, 208, 41–49.
- Besse, J., and V. Courtillot (1991), Revised and synthetic apparent polar wander paths of the African, Eurasian, North American, and Indian plates, and true polar wander since 200 Ma, *J. Geophys. Res.*, 96, 4029–4050.
- Beutler, G., J. Kouba, and T. Springer (1993), Combining the orbits of the IGS processing centers, in *IGS Workshop Proceedings: 1993 IGS Analysis Center Workshop, 12-14 October 1993*, edited by J. Kuba, pp. 20–56, *Geod. Surv. Div.*, Nat. Resour. Can., Ottawa.
- Cattin, R., C. Doubre, J. B. de Chabaliere, G. King, C. Vigny, J. P. Avouac, and J. C. Ruegg (2005), Numerical modelling of quaternary deformation and post-rifting displacement in the Asal-Ghoubbet rift (Djibouti, Africa), *Earth Planet. Sci. Lett.*, 239, 352–367.
- Chu, D., and R. G. Gordon (1999), Evidence for motion between Nubia and Somalia along the Southwest Indian Ridge, *Nature*, 398, 64–67.
- Courtillot, V., A. Galdeano, and J. L. LeMouel (1980), Propagation of an accreting plate boundary: A discussion of new aeromagnetic data in the gulf of Tadjourah and southern Afar, *Earth Planet. Sci. Lett.*, 47, 144–160.
- Dauteuil, O., P. Huchon, F. Quemeneur, and T. Souriot (2001), Propagation of an oblique rift: the western Gulf of Aden, *Tectonophysics*, 332, 423–442.
- de Chabaliere, J. B., and J. P. Avouac (1994), Kinematics of the Asal rift (Djibouti) determined from the deformation of Fieale volcano, *Science*, 265, 1677–1681.
- DeMets, C., et al. (1990), Current plate motions, *Geophys. J. Int.*, 101, 425–478.
- DeMets, C., R. G. Gordon, D. F. Argus, and S. Stein (1994), Effect of recent revisions to the geomagnetic reversal time scale on estimates of current plate motions, *Geophys. Res. Lett.*, 21, 2191–2194.
- Dobre, C., G. Peltzer, I. Manighetti, and E. Jacques (2005), Eight years of surface deformation in the Asal-Ghoubbet rift (Afar depression) observed with SAR data, *Eos Trans. AGU*, 86(52), Fall Meet. Suppl., Abstract G42A-04.
- Fernandes, R. M. S., B. A. C. Ambrosius, R. Noomen, L. Bastos, M. J. R. Wortel, W. Spakman, and R. Govers (2003), The relative motion between Africa and Eurasia as derived from ITRF2000 and GPS data, *Geophys. Res. Lett.*, 30(16), 1828, doi:10.1029/2003GL017089.
- Foulger, G. R., C.-H. Jahn, G. Seeber, P. Einarsson, B. R. Julian, and K. Heki (1992), Post-rifting stress relaxation at the divergent plate boundary in northeast Iceland, *Nature*, 358, 488–490, doi:10.1038/358488a0.



- Herring, T. A., J. L. Davis, and I. I. Shapiro (1990), Geodesy by radio interferometry: The application of Kalman filtering to the analysis of very long baseline interferometry data, *J. Geophys. Res.*, *95*, 12,561–12,581.
- Huchon, P., F. Jestin, J. M. Cantagrel, J. M. Gaulier, S. Al Khirbash, and A. Gafaneh (1991), Extensional deformations in Yemen since Oligocene and the Afar triple junction, *Ann. Tectonicae*, *5*(2), 141–163.
- Jestin, F., P. Huchon, and J. M. Gaulier (1994), The Somalia plate and the East African Rift system: Present day kinematics, *Geophys. J. Int.*, *116*, 637–654.
- King, R. W., and Y. Bock (2000), Documentation for the GAMIT GPS software analysis version 9.9, Mass. Inst. of Technol., Cambridge.
- Le Dain, A. Y., B. Robineau, and P. Tapponnier (1979), Les effets tectoniques de l'événement sismique et magmatique de novembre 1978 dans le rift d'Asal-Ghoubbet, *Bull. Soc. Geol. Fr.*, *7*(6), 817–822.
- Manighetti, I., P. Tapponnier, V. Courtillot, S. Gruszow, and P. Y. Gillot (1997), Propagation of rifting along the Arabia-Somalia plate boundary: The gulfs of Aden and Tadjoura, *J. Geophys. Res.*, *102*, 2681–2710.
- Manighetti, I., P. Tapponnier, P. Y. Gillot, E. Jacques, V. Courtillot, R. Armijo, J. C. Ruegg, and G. King (1998), Propagation of rifting along the Arabia-Somalia plate Boundary: Into Afar, *J. Geophys. Res.*, *103*, 4947–4974.
- Manighetti, I., P. Tapponnier, V. Courtillot, Y. Gallet, E. Jacques, and P. Y. Gillot (2001a), Strain transfer between disconnected, propagating rifts in Afar, *J. Geophys. Res.*, *106*, 13,613–13,665.
- Manighetti, I., G. C. King, Y. Gaudemer, C. H. Scholz, and C. Doubre (2001b), Slip accumulation and lateral propagation of active normal faults in Afar, *J. Geophys. Res.*, *106*, 13,667–13,696.
- McClusky, S., et al. (2000), Global Positioning System constraints on plate kinematics and dynamics in the eastern Mediterranean and Caucasus, *J. Geophys. Res.*, *105*, 5695–5720.
- McClusky, S., R. Reilinger, S. Mahmoud, D. Ben Sari, and A. Tealeb (2003), GPS constraints on Africa (Nubia) and Arabia plate motions, *Geophys. J. Int.*, *155*, 126–138.
- Neilan, R. (1995), The evolution of the IGS global network, current status and future aspects, in *IGS Annual Report*, edited by J. F. Zumberge et al., *JPL Publ.*, *95-18*, 25–34.
- Ruegg, J. C., and M. Kasser (1987), Deformation across the Asal-Ghoubbet rift, Djibouti, uplift and crustal extension 1979–1986, *Geophys. Res. Lett.*, *14*, 745–748.
- Ruegg, J. C., J. C. Lépine, A. Tarantola, and M. Kasser (1979), Geodetic measurements of rifting associated with a seismovolcanic crisis in Afar, *Geophys. Res. Lett.*, *6*, 817–820.
- Ruegg, J. C., F. Gasse, and P. Briole (1990), Mouvements du sol holocènes dans le rift d'Asal à Djibouti, *C. R. Acad. Sci.*, *310*, 1687–1694.
- Ruegg, J. C., et al. (1993), First epoch geodetic GPS measurements across the Afar plate boundary zone, *Geophys. Res. Lett.*, *20*, 1899–1902.
- Sella, G. F., T. H. Dixon, and A. Mao (2002), REVEL: A model for Recent plate velocities from space geodesy, *J. Geophys. Res.*, *107*(B4), 2081, doi:10.1029/2000JB000033.
- Sichler, B. (1980), La biette danakile: Un modèle pour l'évolution géodynamique de l'Afar, *Bull. Soc. Geol. Fr.*, *6*, 925–933.
- Sigmundsson, F. (2006), *Iceland Geodynamics: Crustal Deformation and Divergent Plate Tectonics*, 228 pp., Springer, New York.
- Sigmundsson, F., P. Einarsson, and R. Bilham (1992), Magma chamber deflation recorded by the Global Positioning System, the Hekla 1991 eruption, *Geophys. Res. Lett.*, *19*, 1483–1486.
- Souriot, T., and J. P. Brun (1992), Faulting and block rotation in the Afar triangle East Africa: The Danakil crank arm model, *Geology*, *20*, 911–914.
- Stein, R. S., P. Briole, J. C. Ruegg, P. Tapponnier, and F. Gasse (1991), Contemporary, Holocene and Quaternary deformation of the Asal rift, Djibouti: Implications for the mechanics of slow spreading ridges, *J. Geophys. Res.*, *96*, 21,789–21,806.
- Tapponnier, P., R. Armijo, I. Manighetti, and V. Courtillot (1990), Book-shelf faulting and horizontal block rotations between overlapping rifts in southern Afar, *Geophys. Res. Lett.*, *17*, 1–4.
- Vernant, P., et al. (2004), Contemporary crustal deformation and plate kinematics in Middle East constrained by GPS measurements in Iran and northern Oman, *Geophys. J. Int.*, *157*, 381–398, doi:10.1111/j.1365-246x.2004.02222.x 2004.
- Vigny, C., P. Huchon, J.-C. Ruegg, K. Khanbari, and L. M. Asfaw (2006), Confirmation of Arabia plate slow motion by new GPS data in Yemen, *J. Geophys. Res.*, *111*, B02402, doi:10.1029/2004JB003229.
- Walpersdorf, A., C. Vigny, J.-C. Ruegg, P. Huchon, L. M. Asfaw, and S. Al Khirbash (1999), 5 Years of GPS Observations in the Afar Triple Junction Area, *J. Geodyn.*, *28*(2–3), 225–236.

L. Asfaw, Department of Geophysics, Addis Ababa University, P.O. Box 1176, Addis Ababa, Ethiopia. (observatory.aau@telecom.net.et)

R. Cattin and C. Vigny, Laboratoire de Géologie, ENS, 24 rue Lhomond, 75231, Paris, France. (vigny@geologie.ens.fr)

J.-B. de Chabaliere and J.-C. Ruegg, Laboratoire de Séismotectonique, IPGP, 4 place Jussieu, 75005 Paris, France. (ruegg@ipgp.jussieu.fr)

K. L. Feigl, Department of Geology and Geophysics, University of Wisconsin-Madison, 1215 W Dayton Street, Madison WI 53706, USA. (feigl@wisc.edu)

P. Huchon, Laboratoire de Tectonique, Université Paris VI, 4 place Jussieu, F-75252, Paris, France. (philippe.huchon@lgs.jussieu.fr)

K. Kanbari, Department of Geosciences, Sana'a University, P.O. Box 14433, Sana'a, Yemen. (kkhanbari@hotmail.com)